Correlation Lengths, Inclusive Transverse-Momentum Distributions, and Multiperipheralism*

Se-Yuen Mak and Chung-I Tan
Department of Physics, Brown University, Providence, Rhode Island 02912
(Received 14 January 1972)

Transverse-momentum distributions in the pionization region of the single- and the two-particle inclusive reactions are studied using multiperipheral models. We find that the slope of the diffraction peak for the elastic scattering can be used to set the scale of transverse momenta. The same reasonings also lead to a "broadening" of $\langle q_\perp^2 \rangle$ for the single-particle distribution and to a *positive* correlation, peaking at $\cos\phi = -1$, for the two-particle distribution. The latter effect is due to the existence of a lower J-plane singularity (a branch point for a multi-Regge model), thus having a correlation length $(\alpha_v - \alpha_c)^{-1}$. These general results are then verified by calculations based on an explicit multi-Regge model. We suggest that our predictions are applicable to $a + b \to \pi^+ + \pi^+ +$ anything, and $a + b \to \pi^- + \pi^- +$ anything, where the two detected final particles have exotic quantum numbers.

I. INTRODUCTION

The basic ingredient of the multiperipheral model[1] (MPM) is the neglect of "long-range" correlation effects in particle production at high energies. By incorporating direct-channel unitarity, the integral-equation approach to the MP dynamics allows us to demonstrate explicitly as its consequences the Regge behavior of exclusive processes[1-4] and the scaling properties of inclusive processes.[5,6] These general properties are independent of the detailed nature of the short-range correlations.

Experimentally, it is known that the distribution for the transverse momentum $q_\perp^2$ is roughly exponential. We concentrate in this paper on the consequences of this *experimental input* under the MP considerations. The "central" parameter of our discussion is the average $q_\perp^2$ for elastic scattering, Ω^{-1},[7] defined by

$$\Omega \equiv \left\langle \frac{d}{dt} \ln\left(\frac{d\sigma^{\rm el}}{dt}\right)\right\rangle_{\rm av} . \tag{1.1}$$

In order to avoid the unnecessary complications of solving MP integral equations, we simply assume that the solution has a reasonable spectrum in the J plane – a leading pole at $\alpha_v(0)$, and a branch point at $\alpha_c(0)$, $\alpha_c < \alpha_v$.

We suggest that the MP "chain" structure in general leads to a "broadening" of $\langle q_\perp^2 \rangle$ for the single-particle distribution in the pionization region. We first demonstrate that, for all MPM describable by a Chew-Goldberger-Low (CGL) equation, *our experimental input* implies a large transverse-momentum cutoff of the form

$$f(q_\perp^2) \propto \exp(-\tfrac{1}{2}\Omega q_\perp^2) . \tag{1.2}$$

The same analysis is then used to obtain the large transverse-momentum cutoff for the two-particle production. We find that the deviation from the uncorrelated distribution in the *two-particle pionization* region,

$$\Delta f_{12} \equiv f_{12} - f_1 f_2 ,$$

always contains a *positive* component, which favors the configuration $\cos\phi \equiv \hat{q}_1^\perp \cdot \hat{q}_2^\perp = -1$. Arguments are given that this phenomenon is peculiar to MPM only.

The above qualitative results, obtained by general arguments, are then verified by an explicit calculation using an exponentially damped multi-Regge model (MRM). We find, in particular, that the "correlation function" Δf_{12} is controlled by the branch cut at α_c, and has a large κ_1, κ_2 behavior

$$\Delta f_{12} \propto (\Sigma_{12})^{-(\alpha_v - \alpha_c)} \times \exp\{-\Omega[\tfrac{2}{3}\kappa_1 + \tfrac{2}{3}\kappa_2 + (e^{-y} + \tfrac{2}{3}\cos\phi)(\kappa_1\kappa_2)^{1/2}]\} , \tag{1.3}$$

where $y = y_1 - y_2 > 0$ is the relative rapidity, and

$$\kappa_1 \equiv q_1^{\perp 2} + \mu^2 , \quad \kappa_2 \equiv q_2^{\perp 2} + \mu^2 .$$

As $y \to \infty$, Δf_{12} vanishes as $\exp[-(\alpha_v - \alpha_c)y]$, $\Sigma_{12} \sim 2(\kappa_1\kappa_2)^{1/2}\cosh y$, thus corresponding to a correlation length $(\alpha_v - \alpha_c)^{-1}$. We point out that this positive correlation in the pionization region can best be observed in reactions where two detected particles have exotic quantum numbers.

The concept of a limiting distribution (or scaling)

for inclusive processes can best be described by using Mueller's Regge hypothesis.[8] With the realization that inclusive distributions are directly related to discontinuities of elastic multiparticle scattering amplitudes,[9] it is believed that Mueller's Regge hypothesis is probably on the same footing as the multi-Regge hypothesis[10] for the exclusive processes. In the case of the two-particle distribution,[11] the relevant multiparticle reaction is 4 to 4,

$$p_a + q_1' + q_2' + p_b \to p_a' + q_1 + q_2 + p_b', \tag{1.4}$$

and the discontinuity is always taken in the crossed variable

$$M^2 = (p_a + p_b - q_1 - q_2)^2 . \tag{1.5}$$

The discontinuity $(2i)X_2$, in the forward limit, i.e., $p_a = p_a'$, $q_1 = q_1'$, etc., is schematically represented by Fig. 1(a), and it is related to the two-particle distribution f_{ab}^{12} for the process

$$p_a + p_b \to q_1 + q_2 + \text{anything} \tag{1.6}$$

by

$$f_{ab}^{12} = (\sigma_{ab}^{\text{tot}})^{-1} \Delta^{-1/2}(s, m_a^2, m_b^2) X_2 . \tag{1.7}$$

The Mueller multi-Regge expansions for X_2 in various kinematic regions[11] are illustrated by Figs. 1(b)–1(e). Each diagram corresponds to a limiting distribution for the region in question, and is controlled by the leading vacuum singularity α_v. The shape of the distribution is determined by "coupling functions" associated with vertices, which can only be obtained in models. The contributions from the lower singularities in the complex J plane provide the corrections to the limiting distributions at "nonasymptotic" regions. In particular, these corrections in general do not possess factorization properties of the limiting distributions, thus leading to "short-range" correlation effects.

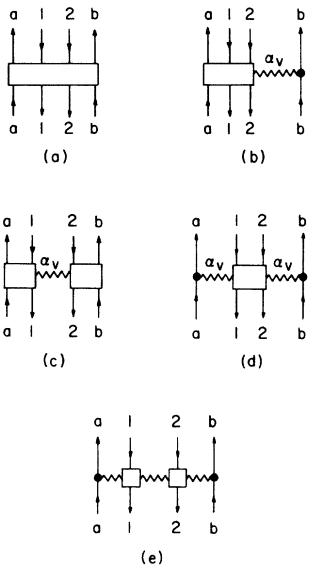

FIG. 1. (a) Mueller diagram for a two-particle inclusive cross section, (b) the limiting distribution for the fragmentation region of particle a, (c) the double-fragmentation limit, (d) the pionization limit, and (e) the uncorrelated pionization limit.

In the CGL model the discontinuity X_2 is given by a sum of eight terms, $A, B, \ldots, H$, corresponding to *different topologies* where the two detected particles are emitted in the MP chain (Figs. 2, 3). From the discussion of Sec. II, it is evident that not all eight MP diagrams contribute to the limiting distributions. By comparing Figs. 1 and 3, we find that the correspondence between the leading Mueller diagrams and the MP diagrams is

Single fragmentation of a:	C, E, G, H	
Single fragmentation of b:	D, F, G, H	
Double fragmentation:	A, B, E, F, H	(1.8)
Correlated pionization:	G, H	
Uncorrelated pionization:	H.	

This correspondence can be established explicitly[6, 12] by a repeated use of the multiperipheral assumptions and by assuming the existence of an isolated leading vacuum singularity α_v. This, in turn, proves the scaling of the two-particle distribution. In particular, it allows us to calculate the "coupling functions" in Mueller expansions in terms of parameters of the MPM.

Diagrams not listed in (1.8) correspond to nonasymptotic corrections. Particular attention is directed to the transition between the correlated and the uncorrelated pionization regions. Under our approximation the diagram H will be factorizable, so that the entire correlation effect in the pionization region is due to the diagram G. This short-range correlation can be shown to correspond to the existence of a J-plane branch point at α_c.[13]

Our program is to first calculate the gross transverse-momenta behavior of the Mueller coupling functions by a general MP consideration. To avoid discussing the details of the MP bootstrap, we shall assume the knowledge of the J-plane singularities at the forward limit and shall ignore the

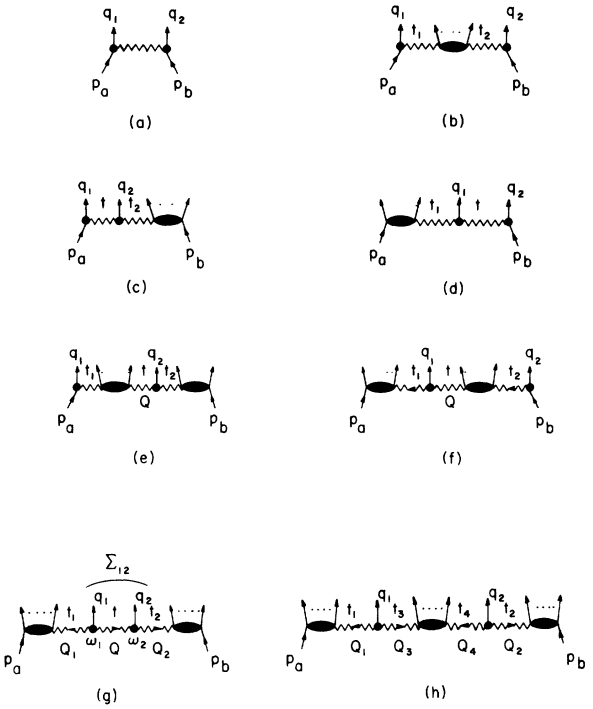

FIG. 2. (a)–(h) Eight inequivalent production configurations in a MP chain.

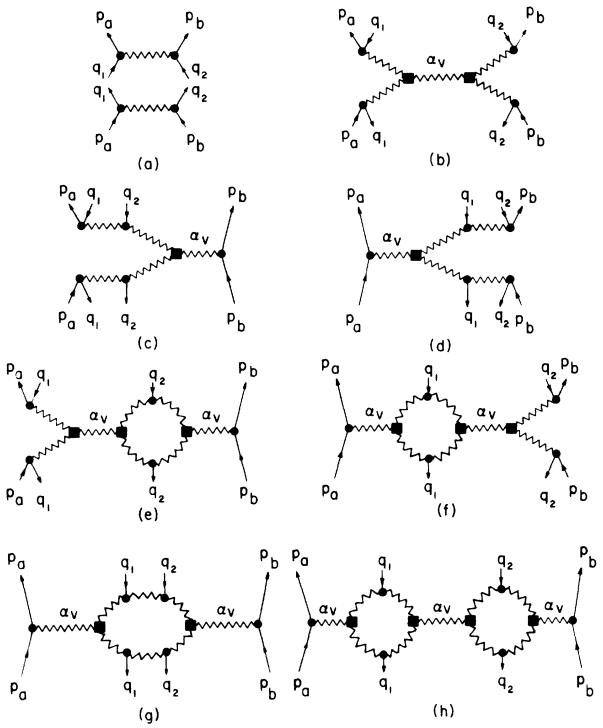

FIG. 3. (a)–(h) Contributions to the Mueller expansion corresponding to the eight MP configurations depicted in Figs. 2(a)–2(h).

effects of Regge slopes. Under these conditions, we find from (1.1) that the elastic amplitude is parametrized by

$$T^{\mathrm{el}}(s,t) \simeq i\gamma(t)(s)^{\alpha_v}\gamma(t), \tag{1.9}$$

where

$$\gamma(t) = ge^{(\Omega/4)t}, \tag{1.10}$$

so that the total cross section is asymptotically given by

$$\sigma^{\mathrm{tot}}(s) \simeq g^2 s^{\alpha_v - 1}. \tag{1.11}$$

The cutoff behavior (1.2) and (1.3) can then be shown to follow from the "chain" structure of the CGL model. In order to make our discussions self-contained, we review briefly the structure of the CGL model and the scaling property of the two-particle distribution in Sec. II. Transverse-momentum cutoffs for the single- and the two-particle distributions are derived in Sec. III. In Sec. IV, we obtain explicit representations for X_2, using an exponentially damped MRM, which not only verify results of Sec. III, but also provide us with distribution functions for other kinematic regions. Finally, we examine the generality of our results in Sec. V.

II. KINEMATICS OF THE CGL MODEL AND SCALING

A. Single-Particle Distribution in the CGL Model

The single-particle distribution function f_{ab}^1 is defined by

$$f_{ab}^1 \equiv (\sigma_{ab}^{\mathrm{tot}})^{-1}(2E)\frac{d\sigma}{d^3q}$$
$$= (\sigma_{ab}^{\mathrm{tot}})^{-1}\Delta^{-1/2}(s, m_a^2, m_b^2)X_1, \tag{2.1}$$

where X_1 is the discontinuity of a 3-to-3 amplitude in $M^2 = (p_a + p_b - q)^2$, and Δ is the usual triangle function. By making a multi-Regge expansion for production amplitudes, X_1 is calculated by integrating over the final-state phase space and summing over the number of produced particles. It is then given by a sum of three terms, corresponding to inequivalent production configurations in a MP chain. Each term involves one or two ladder sums, which can always be related to the solution of a MP integral equation (the CGL equation in the present case). In the pionization region, we find [Fig. 4(a)]

$$X_1(p_a; q; p_b) \simeq \frac{2}{(2\pi)^7} \int d^4Q_1\, d^4Q_2\, \delta^4(Q_1+Q_2+q) B_l(p_a; +Q_1, -Q_2) |\beta(t_1, \omega, t_2)|^2 B_r(-Q_1, +Q_2; p_b). \quad (2.2)$$

The derivation of (2.2) can be found in I and II, and we follow closely notations introduced there: Σ's always refer to subenergies between neighboring particles, t's are momentum transfers squared inside a MP chain, ω's are Toller angles, $\gamma(t)$ and $\beta(t, \omega, t')$ are the single- and the double-Regge couplings, respectively. B_l and B_r, the auxiliary absorptive parts, are solutions of the CGL equation. The Regge factor $H(\Sigma, t)$, which enters in the buildup of B's, is parametrized by $(\Sigma/\mu^2)^{\alpha(t)}$, where $\alpha(t)$ is the input Regge pole. [See Fig. 4(b).]

B. Two-Particle Distribution in the CGL Model

Similarly, the two-particle distribution for the process (1.4) is related to the invariant cross section by

$$f_{ab}^{12} = (\sigma_{ab}^{\text{tot}})^{-1}(2E_1)(2E_2)\frac{d\sigma}{d^3q_1 d^3q_2}$$

$$= (\sigma_{ab}^{\text{tot}})^{-1}\Delta^{-1/2}(s, m_a^2, m_b^2) X_2. \quad (2.3)$$

In the MPM, X_2 is given by a sum of eight terms,

$$X_2 = A + B + \cdots + H, \quad (2.4)$$

corresponding to the MP configurations illustrated in Fig. 2. Again, using the MR expansion and performing the ladder sums, we find that each diagram in Fig. 2 can be expressed in terms of B's. For example, the diagram G is given by

$$G = \frac{2}{(2\pi)^{10}} \int d^4Q_1 d^4Q d^4Q_2\, \delta^4(Q_1+Q+q_1)\delta^4(Q_2-Q+q_2) B_l(p_a; Q_1, -Q)$$
$$\times |\beta(t_1, \omega_1, t)|^2 |H(t, \Sigma_{12})|^2 |\beta(t, \omega_2, t_2)|^2 B_r(Q, Q_2; p_b), \quad (2.5)$$

where $t = Q^2$, $t_1 = Q_1^2$, $t_2 = Q_2^2$. The derivation of (2.5) and the representations for the rest of Fig. 2 are given in Appendix A.

f_{ab}^{12}, in general, depends on six independent variables,[12] which can be chosen to be $s = (p_a+p_b)^2$, y_1, y_2, $q_1^\perp$, $q_2^\perp$, and $\cos\phi = \hat{q}_1^\perp \cdot \hat{q}_2^\perp$. ($y$'s are the rapidities. Our convention is $y_a \geq y_1 \geq y_2 \geq y_b$.) However, for our subsequent discussions, it is often convenient to use invariants. They include

Energy variables:

$$s, \Sigma_{12} = (q_1+q_2)^2, \quad M^2 = (p_a+p_b-q_1-q_2)^2,$$
$$M_1^2 = (p_a+p_b-q_1)^2, \quad M_2^2 = (p_a+p_b-q_2)^2, \quad (2.6)$$
$$\kappa_1 \equiv \mu^2 + q_1^{\perp 2}, \quad \kappa_2 \equiv \mu^2 + q_2^{\perp 2}.$$

Momentum transfers:

$$u_1 = (p_a-q_1)^2, \quad u_2 = (p_a-q_2)^2,$$
$$v_1 = (p_b-q_1)^2, \quad v_2 = (p_b-q_2)^2. \quad (2.7)$$

One useful relation among these variables is

$$\Sigma_{12} = 2\mu^2 + 2(\kappa_1\kappa_2)^{1/2}\cosh y - 2q_1^\perp q_2^\perp \cos\phi \quad (y \equiv y_1 - y_2). \quad (2.8)$$

C. Scaling of the Two-Particle Distribution

The general multiperipheral assumption of strong dampings for all momentum transfers, together with the assumption of the Pomeranchukon dominance of the B's, are sufficient to demonstrate the scaling of f_{ab}^{12} in a manner completely analogous to the treatment of f_{ab}^1 in II. The MP assumption allows us to show that phase-space integrations for $A, \ldots, H$ scale, and the dominant contributions of the integrands always come from regions where either B's already have the correct variable dependences or their behavior is known. Because of the "scaling" property[1-4] of the kernel of the CGL equation, it generally follows that B

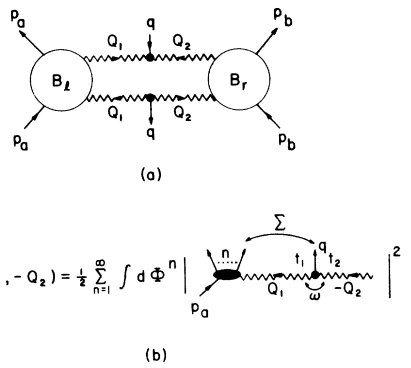

FIG. 4. (a) The pionization limit of a single-particle inclusive cross section, and (b) the multiperipheral summation for the CGL auxiliary function.

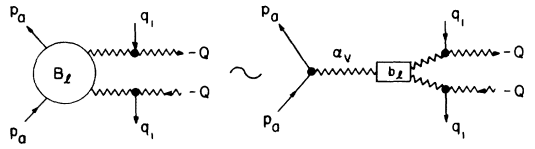

FIG. 5. Schematic representation of the Regge behavior of the CGL B function.

has Regge behavior (Fig. 5), i.e., as s_1', s_1, s_2', $s_2 \to \infty$,

$$B_l(p_a; -Q-q_1, -Q) \simeq (s_1')^{\alpha_v} b_l(s_1/s_1', t_1), \tag{2.9}$$

$$B_r(Q, Q-q_2; p_b) \simeq (s_2')^{\alpha_v} b_r(s_2/s_1', t_2), \tag{2.10}$$

where

$$s_1' = (-Q-q_1+p_a)^2, \quad s_1 = (-Q+p_a)^2,$$
$$s_2' = (Q-q_2+p_b)^2, \quad s_2 = (Q+p_b)^2, \tag{2.11}$$

and

$$t = Q^2, \quad t_1 = (Q+q_1)^2, \quad t_2 = (Q-q_2)^2.$$

It can then be shown that the terms listed in (1.8) always have asymptotic behavior, s^{α_v}, with coefficients which are functions of scaled variables only. Next we assume that α_v is the same vacuum singularity which controls the total cross section, (1.11); the scaling property of f_{ab}^{12} then follows. Since the demonstration of the above arguments is straightforward, we shall not present it here. However, certain technical details are given in Appendix B. To summarize: We replace each ladder sum by a vacuum Regge pole α_v,[13] thus arriving at Figs. 3(a) through 3(h), representing contributions A through H, respectively.

III. TRANSVERSE-MOMENTUM CUTOFF IN THE PIONIZATION REGION

The scaling property[14] of the single-particle distribution for the general MPM has been demonstrated in II, and an explicit form of the distribution has also been obtained in I for a MRM with exponential damping in momentum transfers. By combining the approaches of I and II, we next obtain qualitative features of transverse-momentum cutoffs and correlations for the single- and the two-particle distributions that follow from the general "chain" structure MPM. However, to make our discussion precise, we shall restrict ourselves to those MPM describable by CGL equations. As we have already noted in Ref. 1, with proper interpretation, all MPM studied so far can be considered as special cases of CGL models. Therefore, we believe that the conclusions of this section are of general validity.

We first apply our procedure to the single-particle case, where explicit results are known for special cases. We next treat the two-particle distribution in the pionization region.

A. Single-Particle Distribution

Separating $d^2Q_1^\perp$, $d^2Q_2^\perp$ from d^4Q_1, d^4Q_2, we find that X_1 in (2.2) can be written as [also use (2.9) and (2.10)]

$$X_1 = \frac{(2)(\kappa)^{\alpha_v}(s)^{\alpha_v}}{(2\pi)^7} \int dx dz d^2Q_1^\perp d^2Q_2^\perp \, \delta^2(\vec{Q}_1^\perp + \vec{Q}_2^\perp + \vec{q}_\perp) \times b_l(x, t_1) |\beta(t_1, \omega, t_2)|^2 b_r(z, t_2), \tag{3.1}$$

where

$$x \equiv p_a \cdot Q_1 / p_a \cdot q, \quad z \equiv p_b \cdot Q_2 / p_b \cdot q,$$

and

$$\kappa \equiv \frac{2(p_a \cdot q)(p_b \cdot q)}{p_a \cdot p_b} \simeq q_\perp^2 + \mu^2. \tag{3.2}$$

Using the MP hypothesis of strong damping in t_1 and t_2, we find (see II),

$$t_1 \simeq -Q_1^{\perp 2} - \kappa(z+1)x + O(1/s), \tag{3.3a}$$

$$t_2 \simeq -Q_2^{\perp 2} - \kappa(x+1)z + O(1/s), \tag{3.3b}$$

and the dominant contribution in (3.1) comes from $0 < x \lesssim O(1)$, $0 < y < O(1)$. Any $Q_1^{\perp 2}$ and $Q_2^{\perp 2}$ dependence in (3.1) will only come from t_1 and t_2 via (3.3).

We first generalize the t cutoff for the single-Regge coupling, (1.10), to the MP chain. By factorization, we expect a similar factor associated with each internal momentum-transfer variable. For definiteness, we approximate

$$\beta(t, \omega, t_2) \simeq \gamma(t_1) \tilde{\beta} \gamma(t_2), \tag{3.4}$$

where $\tilde{\beta}$ is assumed to be smooth,[15] and later will be set to be $\gamma(\mu^2)^{-1}$. This rapid damping in t's can be shown to survive the ladder summation (see I), e.g.,

$$B_l(s_1, s_1', t_1) \sim (s_1')^{\alpha_v} \tilde{b}_l(x) \gamma^2(t_1)$$

and (3.5)

$$\tilde{b}_l(x) \propto x^{2\bar{\alpha}},$$

where $\bar{\alpha}$ is taken to be the average $\alpha(t_1)$, $\bar{\alpha} \simeq \alpha(0)$. Independent of this specific assumption, we find

$$X_1 \sim s^{\alpha_v} \int dx dz d^2Q_1^\perp d^2Q_2^\perp \, \delta^2(\vec{Q}_1^\perp + \vec{Q}_2^\perp + \vec{q}_\perp) \times e^{\Omega(t_1+t_2)} I(x, z, \ldots), \tag{3.6}$$

where $I(x, z, \ldots)$ is a smooth function.

The important observation to be made is that in

order for $q_\perp{}^2$ to be large, either $Q_1^{\perp 2}$ or $Q_2^{\perp 2}$ (or both) has to increase, which then forces $|t_1|$, $|t_2|$ to grow. However, because of the presence of $\exp[\Omega(t_1+t_2)]$, and the conditions (3.3a) and (3.3b), we find that the large $q_\perp{}^2$ behavior gets most of its contribution from $0<x,\ z\ll 1$. (That is, $0<s_1'/s_1 \ll 1$ and $0<s_2'/s_2\ll 1$, yet s_1' and s_2' are still allowed to be large.) We are then left with

$$X_1 \sim \int d^2Q_1^\perp d^2Q_2^\perp\, \delta^2(\vec{Q}_1^\perp+\vec{Q}_2^\perp+\vec{q}_\perp) \times \exp[-\Omega(Q_1^{\perp 2}+Q_2^{\perp 2})]\,. \tag{3.7}$$

For $q_\perp{}^2\to\infty$, an asymptotic estimate yields

$$X_1 \propto \exp[-\Omega|\,Q_1^{\perp 2}+Q_2^{\perp 2}|_{\min}] = \exp(-\tfrac{1}{2}\Omega q_\perp{}^2)\,, \tag{3.8}$$

corresponding to the configuration

$$\vec{Q}_1^\perp=\vec{Q}_2^\perp=-\vec{q}_\perp/2\,. \tag{3.9}$$

Our crude calculation above agrees with the explicit calculation in I,[16] and a similar result has also been obtained by Bali, Pignotti, and Steele of Ref. 6. We believe that this "broadening" of $\langle q_\perp{}^2\rangle$ is a general consequence of any MPM with rapid damping in t's. The origin of the broadening effect is the "sharing" of $\vec{q}_\perp$ by two adjacent t's in a MP chain. It is interesting to note that experimentally[7] Ω ranges from 6 to 10 $(\mathrm{GeV}/c)^{-2}$, whereas the single-particle distribution has an observed pionization cutoff[17] [in $(\mathrm{GeV}/c)^{-2}$]

$$\exp(-3.5q_\perp{}^2)\,. \tag{3.10}$$

We would also like to point out that calculations[18] based on the dual-resonance model have yielded a cutoff behavior, $\exp(-4\alpha' q_\perp{}^2)$, $\alpha'\simeq 1\ (\mathrm{GeV}/c)^{-1}$, whereas the elastic large angle (e.g., $\theta_{\mathrm{c.m.}}=\pi/2$) cutoff is $\exp(-8\ln 2\,\alpha' q_\perp{}^2)$. However, we do not see any obvious connections between these two results.

B. Two-Particle Distribution

It follows from (1.8) that, for the pionization region, we only need to consider diagrams G and H. Under our approximation[13] (2.9) and (2.10), H is factorized (Appendix D), so that the cutoff in $\vec{q}_1^\perp$ and $\vec{q}_2^\perp$ is

$$H \propto \exp(-\tfrac{1}{2}\Omega q_1^{\perp 2})\exp(-\tfrac{1}{2}\Omega q_2^{\perp 2}) = \exp[-\tfrac{1}{2}\Omega(q_1^{\perp 2}+q_2^{\perp 2})]\,, \tag{3.11}$$

and the correlation effect is entirely contained in G. Following the procedure of Sec. III A, we first introduce

$$x=\frac{p_a\cdot Q_1}{p_a\cdot(q_1+q_2)}\,,\quad z=\frac{p_b\cdot Q_2}{p_a\cdot(q_1+q_2)}\,, \tag{3.12}$$

and find from (2.5) that the large $q_1^\perp$, $q_2^\perp$ contribution can be written as

$$G\sim\int dx\int dz\int d^2Q_\perp \exp[\Omega(t_1+t+t_2)]I'(x,z,\ldots)\,, \tag{3.13}$$

where I' is a smooth function, and

$$Q_1^{\perp 2}\simeq -t_1-[\kappa_1+\kappa_2+2(\kappa_1\kappa_2)^{1/2}\cosh y](z+1)x\,, \tag{3.14a}$$

$$Q_\perp{}^2\simeq -t-(\kappa_1\kappa_2)^{1/2}e^{-y}[x(1+e^y)+1][z(1+e^y)+1]\,, \tag{3.14b}$$

$$Q_2^{\perp 2}\simeq -t_2-[\kappa_1+\kappa_2+2(\kappa_1\kappa_2)^{1/2}\cosh y](x+1)z\,, \tag{3.14c}$$

$\kappa_i\equiv q_i^{\perp 2}+\mu^2$, $i=1,2$ and $\vec{Q}_1^\perp=-(\vec{Q}_\perp+\vec{q}_1^\perp)$, $\vec{Q}_2^\perp=\vec{Q}_\perp-\vec{q}_2^\perp$. In the limit κ_1,κ_2 large, $|t_1+t+t_2|_{\min}$ occurs at $0\simeq y,\ z\ll 1$, so that we are left with

$$G\propto\exp\{-\Omega[\kappa_1+\kappa_2+(\kappa_1\kappa_2)^{1/2}e^{-y}]\} \times\int d^2Q_\perp\exp\{-\Omega[3Q_\perp{}^2+2\vec{Q}_\perp\cdot(\vec{q}_1^\perp-\vec{q}_2^\perp)]\}\,. \tag{3.15}$$

A saddle-point calculation indicates that the least damping occurs at $\vec{Q}_\perp=-\frac{1}{3}(\vec{q}_1^\perp-\vec{q}_2^\perp)$, and

$$G\propto\exp\{-\Omega[\tfrac{2}{3}q_1^{\perp 2}+\tfrac{2}{3}q_2^{\perp 2}+(e^{-y}+\tfrac{2}{3}\cos\phi)q_1^\perp q_2^\perp]\}\,. \tag{3.16}$$

Since contributions from both G and H are positive, we find from (3.11) and (3.16) that the distribution $f_{12}(q_1^\perp, q_2^\perp, \cos\phi, y)$ is monotonic in $\cos\phi$ and has a maximum at $\phi=\pi$, for y, $q_1^\perp$, $q_2^\perp$ fixed. Furthermore, consider the case $e^{-y}<\frac{2}{3}$, and say $q_1^\perp$ is large, it follows from (3.16) that the most probable distribution from Δf_{12} is $q_2^\perp=\frac{1}{2}(1-\frac{3}{2}e^{-y})\,q_1^\perp$ and $\phi=\pi$. That is, whenever a particle with a large transverse momentum is detected, it is most likely to find another particle also with large transverse momentum, but pointing in the opposite direction (of course, we need to first subtract the uncorrelated distribution).

C. Discussion

Equations (3.8) and (3.16) are admittedly consequences of our specific approximations leading to Eqs. (3.6) and (3.13). However, we do not really need to require either Toller-angle independence or factorization of internal couplings, but rather assume that the *dominant* damping factors be given by (3.7) and (3.15). Since these dependences arise naturally through the *chain* structure of MPM, we thus believe the qualitative features derived above are general. Therefore, we suggest that the pres-

ence of *a positive correlation in the pionization region favoring* $\cos\phi = -1$ indicates the presence of "multiperipheralism."

It is clear that this effect, if present, is *not* a consequence of the over-all energy momentum conservation, but rather indicates a local effect that is dynamical. This is also to be contrasted with the "independent emission model" where one expects isotropy in ϕ. In both cases, there will be no long-range correlation so that Δf_{12} will diminish as we increase the relative rapidity y in the central region. From Mueller's Regge expansion, we expect that the rate of decrease of Δf_{12} will be controlled by the "gap" between α_v and the next dominant J-plane singularity. In the CGL model, this will be a branch point at $\alpha_c = 2\alpha_0 - 1$.

IV. RESULTS OF AN EXPONENTIALLY DAMPED MULTI-REGGE MODEL

The two-particle distribution is obtained using a concrete model which assumes Regge behavior in cluster energies and exponential damping in the MP momentum transfers. The model is basically the same as that first considered by Caneschi and Pignotti,[19] and as explained in I, we have been able to carry out *analytic* calculations without having to approximate phase-space factors. Under the assumption of a rapid exponential damping in t: $\gamma(t) = g\exp(\frac{1}{4}\Omega t)$, $\beta(t, \omega, t') = \gamma(\mu^2)^{-1}\gamma(t)\gamma(t')$, the CGL integral equation can be approximated by a separable kernel; and we obtain

$$B_r(Q, Q_2; p_b) \simeq g^2\left[\frac{(Q+p_b)^2}{(Q_2+p_b)^2}\right]^{2\alpha(t_2)} \frac{|\gamma(t_2)|^2}{|\gamma(\mu^2)|^2}[(Q_2+p_b)^2]^{\alpha_v} \tag{4.1}$$

in terms of which diagrams $A, \ldots, H$ can be calculated. For instance, it follows from (4.1) and (2.6) that

$$G = \frac{2}{(2\pi)^{10}} g^8 e^{-2\Omega\mu^2} \int d^4Q\, e^{\Omega(t_1+t+t_2)}(s_1')^{\alpha_v}(s_1/s_1')^{2\bar{\alpha}_1}(\Sigma_{12}/\mu^2)^{2\bar{\alpha}_0}(s_2/s_2')^{2\bar{\alpha}_2}(s_2')^{\alpha_v}\,, \tag{4.2}$$

where we have replaced α_i by an average value $\bar{\alpha}_i \simeq \alpha_i(0)$. This integral can actually be integrated to yield (Appendix C)

$$G = g^8 e^{-2\Omega\mu^2}(M^2)^{\alpha_v}(\Sigma_{12}/\mu^2)^{2\bar{\alpha}_0-1-\alpha_v}\Phi_{\alpha_1,\alpha_2}(c, a_1, a_2, b)\,, \tag{4.3}$$

where $\Phi_{\alpha_1,\alpha_2}(c, a_1, a_2, b)$ is given by Eq. (C19).

Equation (4.1) also allows us to write down diagrams C and D directly and to show that H is precisely a product of two single-particle distributions derived in I (Appendix D). Explicit expressions for E and F can be obtained similarly, whereas A is simply the nonforward elastic scattering cross section. In what follows, we first describe the properties of the diagram G in various kinematic regions and then comment on the features of other diagrams.

A. Correlation in the Pionization Region

In this limit, we have $M^2/s \to 1$ and

$$\begin{aligned}
&c - a_1 \simeq -\Omega(2v_2 + v_1) \to \infty\,, \quad c - a_2 \simeq -\Omega(2u_1 + u_2) \to \infty\,,\\
&a_1 + a_2 \simeq 3\Omega M^2 \simeq 2b \simeq 2c \to \infty\,,\\
&b - c \simeq -\tfrac{1}{3}\Omega[6(\kappa_1\kappa_2)^{1/2}e^{-y} + 3(\kappa_1\kappa_2)^{1/2}e^{y} + 2(\kappa_1+\kappa_2) - 2(2q_1^{\perp}q_2^{\perp}\cos\phi + 2\mu^2)]\,,\\
&\lambda = \frac{(c-a_1)(c-a_2)}{a_1+a_2} \simeq \frac{2\Omega}{3}[\kappa_1 + \kappa_2 + 2(\kappa_1\kappa_2)^{1/2}(e^{-y} + \tfrac{1}{4}e^{y})]\,.
\end{aligned} \tag{4.4}$$

We can demonstrate that (a) Φ_{α_1,α_2} reaches a limiting distribution, i.e., $\Phi_{\alpha_1,\alpha_2} \to \Phi_{\alpha_1,\alpha_2}(y, \kappa_1, \kappa_2, \cos\phi)$; (b) as $y \to \infty$, $\Phi_{\alpha_1,\alpha_2}(\infty, \kappa_1, \kappa_2, \cos\phi) \neq 0$ and finite, so that

$$\Delta f^{12} \propto G/s^{\alpha_v} \propto (\Sigma_{12})^{-(\alpha_v-\alpha_c)} \sim \exp[-(\alpha_v - \alpha_c)y]\,, \tag{4.5}$$

where $\alpha_c \equiv 2\bar{\alpha}_0 - 1$ is the leading vacuum branch point. Equation (4.5) indicates that the branch cut contributes a short-range correlation with a correlation length $(\alpha_v - \alpha_c)^{-1}$.

The analytic form of Φ_{α_1,α_2} can be given in terms of elementary functions in the physically interesting cases of $\bar{\alpha}_1, \bar{\alpha}_2 = 0$ or $\frac{1}{2}$ through the use of Eq. (C11). However, since we are primarily interested in the gross correlation effect, e.g., the large transverse-momentum cutoff, we allow α_1, α_2 to be arbitrary and consider the limit

$$s \gg \kappa_1 \gg \mu^2, \quad s \gg \kappa_2 \gg \mu^2. \tag{4.6}$$

(More precisely, the limit $\kappa_i/s, \mu^2/\kappa_i \to 0$, $i=1,2$.) In this case,

$$\frac{\lambda}{\Omega\Sigma_{12}} \simeq \frac{1}{3}\frac{\kappa_1+\kappa_2+2(\kappa_1\kappa_2)^{1/2}(e^{-y}+\frac{1}{4}e^{y})}{(\kappa_1\kappa_2)^{1/2}(\cosh y-\cos\phi)},$$

$$\frac{M^2}{c} \simeq \frac{2}{3}\frac{1}{\Omega}, \tag{4.7}$$

$$\tau_1(c-a_1) \simeq \Omega[2(\kappa_1\kappa_2)^{1/2}e^{-y}+\kappa_1],$$

$$\tau_2(c-a_2) \simeq \Omega[2(\kappa_1\kappa_2)^{1/2}e^{-y}+\kappa_2],$$

and

$$-b+c+\Omega(\Sigma_{12}-2\mu^2) \simeq -\Omega[\tfrac{2}{3}(q_1^{\perp 2}+q_2^{\perp 2})+(e^{-y}+\tfrac{2}{3}\cos\phi)(\kappa_1\kappa_2)^{1/2}]. \tag{4.8}$$

Using $\sigma_{\text{tot}} \simeq g^2 s^{\alpha_v - 1}$, we obtain from (C21) and (1.7) that

$$\Delta f^{12} \sim \frac{g^6 e^{-2\Omega\mu^2}}{12(2\pi)^9\Omega}\Gamma(\alpha_v-(2\bar{\alpha}_1-1))\Gamma(\alpha_v-(2\bar{\alpha}_2-1))\left[\frac{2(\kappa_1\kappa_2)^{1/2}(\cosh y-\cos\phi)}{\mu^2}\right]^{2\bar{\alpha}_0}$$

$$\times\{2\Omega^2[\kappa_1+\kappa_2+2(\kappa_1\kappa_2)^{1/2}e^{-y}+\tfrac{1}{2}(\kappa_1\kappa_2)^{1/2}e^{y}]\}^{-\alpha_v-1}\{\Omega[2(\kappa_1\kappa_2)^{1/2}e^{-y}+\kappa_1]\}^{2\bar{\alpha}_1}$$

$$\times\{\Omega[2(\kappa_1\kappa_2)^{1/2}e^{-y}+\kappa_2]\}^{2\bar{\alpha}_2}\exp\{-\Omega[\tfrac{2}{3}(q_1^{\perp 2}+q_2^{\perp 2}+q_1^{\perp}q_2^{\perp}\cos\phi)+e^{-y}(\kappa_1\kappa_2)^{1/2}]\}. \tag{4.9}$$

Comparing (4.9) with (3.16), we find that the large κ_1, κ_2 behavior is precisely that given by the general MP arguments. Our explicit calculation has furnished us with further information on the correlation length, as well as a detailed correlation function.

B. Single Fragmentation of a

This region can best be described by Feynman's scaled variables $x_1 \equiv q_1^{\parallel}/q_{\max}$, $x_2 = q_2^{\parallel}/q_{\max} > 0$, in the c.m. system of a, b. With our convention $q_1^{\parallel} > q_2^{\parallel}$, for $q_1^{\perp}$, $q_2^{\perp}$ finite, energy conservation requires $x_1 > x_2$, and $1 \geq x_1 \geq 0$, $1 - x_1 \geq x_2 \geq 0$. In this case, we find that

$$c - a_2 \simeq f(x_1, x_2, \kappa_1, \kappa_2) \tag{4.10}$$

is finite, and

$$\begin{aligned} c - a_1 &\simeq \Omega s(2x_2 + x_1), \\ a_1 + a_2 &\simeq 3\Omega s(1 - x_1 - x_2), \end{aligned} \tag{4.11}$$

so that G contributes to the distribution f_a^{12} an amount

$$\Delta f_a^{12} \simeq (\Sigma_{12}/\mu^2)^{-(\alpha_v-\alpha_c)} \times e^{-\Omega Y}\Phi'_{\alpha_1,\alpha_2}(x_1, x_2, q_1^{\perp}, q_2^{\perp}, \phi), \tag{4.12}$$

where

$$Y = \frac{2x_1+3x_2-x_2^2}{x_1(3-2x_1-x_2)}\kappa_1 - \frac{2-x_1}{3-2x_1-x_2}\kappa_2 - \frac{2(1+x_1)}{3-2x_1-x_2}q_1^{\perp}q_2^{\perp}\cos\phi, \tag{4.13}$$

$$\Sigma_{12} \simeq 2\mu^2 + \left(\frac{x_2}{x_1}\right)\kappa_1 + \left(\frac{x_1}{x_2}\right)\kappa_2 - 2q_1^{\perp}q_2^{\perp}\cos\phi. \tag{4.14}$$

Equation (4.12) indicates that Δf_a^{12} reaches a limiting distribution, and it vanishes when $x_1/x_2 \gg 1$, $\Sigma/\mu^2 \to \infty$. Equation (4.13) indicates that an exponential cutoff in κ_1 and κ_2 also exists where coefficients depend on x_1, x_2 and $\cos\phi$. This is to be contrasted with the contribution from the diagram H [Eq. (4.10) of I],

$$\exp\left[-\Omega\left(\frac{1}{2-x_1}\kappa_1+\frac{1}{2-x_2}\kappa_2\right)\right]. \tag{4.15}$$

Together we find that the damping is again most effective at $\phi = 0$, and the angle $\phi = \pi$ is preferred. In the limit $x_1, x_2 \to 0$, and

$$x_2/x_1 \to (\kappa_2/\kappa_1)^{1/2}e^{-y}. \tag{4.16}$$

Equation (4.12) reduces to Eq. (4.19), i.e., the fragmentation region smoothly approaches the pionization region. It also follows from (4.12) that the correlation length coming from G is again $(\alpha_v - \alpha_c)^{-1}$.

C. Deep-Inelastic Region

This region is characterized by $|\vec{q}_1| = O(\sqrt{s})$, $|\vec{q}_2| = O(\sqrt{s})$ in the c.m. system. It has been shown in the case of the single-particle production that the distribution has an exponential cutoff [Eq. (4.5) of I]

$$f_{ab}^{i} \sim \exp\{-s\Omega[(1-\tfrac{1}{2}r) - [(1-\tfrac{1}{2}r)^2 - \tfrac{1}{4}r^2\sin\theta]^{1/2}]\} \quad (\theta \neq 0), \quad (4.17)$$

where $r = q_0/q_{\max}$, $q_{\max} = \sqrt{s}/2$, $\sin\theta \simeq q^{\perp}/q_0$. A similar cutoff has also recently been obtained by Huang and Segrè using the dual-resonance model (DRM).[20] Strictly speaking, neither model is really applicable in this region where cross sections are extremely small. However, it is interesting to note that in both the DRM and the MPM, the behavior in this region and the cutoff in the pionization region are smoothly connected.

It can easily be shown that Eq. (C21) is still applicable in this case. Introducing, in the c.m. system ($q_{\max} = \sqrt{s}/2$),

$$r_{\perp} = q_1^0/q_{\max}, \quad r_2 = q_2^0/q_{\max}, \quad (4.18)$$

$$z_1 = \cos\theta_1 = \hat{q}_1 \cdot \hat{z}, \quad z_2 = \cos\theta_2 = \hat{q}_2 \cdot \hat{z}, \quad z_{12} \equiv \hat{q}_1 \cdot \hat{q}_2, \quad (4.19)$$

we find that the dominant cutoff is of the form

$$\Delta f_{12} \propto \exp[-s\Omega J(r_1, r_2, z_1, z_2, z_{12})], \quad (4.20)$$

where

$$J = \frac{1}{s}\left(\frac{b-c}{\Omega} - \Sigma\right),$$

$$\frac{b}{s\Omega} = \tfrac{1}{2}[3 - \tfrac{3}{2}(r_1+r_2) - \tfrac{1}{2}(r_1z_1 - r_2z_2) + \tfrac{3}{2}r_1r_2(1-z_{12})],$$

$$\frac{c}{s\Omega} = \left\{\left(\frac{b}{s\Omega}\right)^2 - [2r_1(1-z_1)+r_2(1-z_2)][2r_2(1+z_2)+r_1(1+z_1)] - 4r_1r_2(1-z_{12})[1-r_1-r_2+\tfrac{1}{2}r_1r_2(1-z_{12})]\right\}^{1/2}, \quad (4.21)$$

$$\frac{\Sigma}{s} = \frac{r_1r_2}{2}(1-z_{12}).$$

Together with the fact that H is a product of two factors of the form (4.17), we see that f^{12} scales in the same manner as in the single-particle case.

D. Other Diagrams

As we have already mentioned, the diagram H can be decomposed into a product of two single-particle distributions, which, according to Eq. (1.8), contributes to all kinematic regions except at the boundary of the phase space. Near the boundary, end diagrams A, B, C, D, E, and F are important, leading to various types of triple-Regge behavior. For instance, at $x_1 + x_2 \simeq 1$, $x_1 > x_2$, we find

$$C \sim g^6 e^{2\Omega\mu^2} s^{\alpha_v} \left(\frac{\Sigma}{\mu^2}\right)^{2\bar{\alpha}_0} (1-x_1-x_2)^{\alpha_v - 2\bar{\alpha}_2} (1-x_1)^{2\bar{\alpha}_2} h, \quad (4.22)$$

$$h = \left(\frac{1}{2\pi}\right)^6 \exp\left\{-\Omega\left[(\kappa_1)\left(\frac{2-x_2}{x_1}\right) + (\kappa_2)\left(\frac{1-\kappa_1}{x_2}\right) + 2q_1^{\perp}q_2^{\perp}\cos\phi - m^2(2-2x_1-x_2)\right]\right\}. \quad (4.23)$$

Diagram D has a similar behavior at $x_1 + x_2 \simeq -1$. In the di-triple-Regge limit where $x_1 \simeq 1$, $x_2 \simeq -1$, the diagram B gives a contribution

$$B \sim g^6 e^{-\Omega\mu^2} s^{\alpha_v} (1-x_1)^{\alpha_v - 2\bar{\alpha}_1} (1+x_2)^{\alpha_v - 2\bar{\alpha}_2} h', \quad (4.24)$$

$$h' = (2\pi)^{-6} \exp\{-\Omega[\kappa_1/x_1 - \mu^2 - m^2(1-x_1)]\} \exp\{-\Omega[\kappa_2/x_2 - \mu^2 - m^2(1+x_2)]\}. \quad (4.25)$$

In this limit, the rest of the diagrams can all be shown to vanish relative to B, so that the distribution is independent of the angle ϕ – another reflection of the short-range correlation of the MPM.[21-23] Diagrams E and F are factorizable, and they are given respectively by

$$E = \frac{g^8}{(2\pi)^3} \exp(\Omega\mu^2/2) \exp\{-\Omega[\kappa_1/x_1 - m^2(1-x_1)]\} (1-x_1)^{\alpha_v - 2\bar{\alpha}} X_1(p_a; q_2; p_b),$$

$$F = \frac{g^8}{(2\pi)^3} \exp(\Omega\mu^2/2) \exp\{-\Omega[-\kappa_2/x_2 - m^2(1+x_2)]\} (1+x_2)^{\alpha_v - 2\bar{\alpha}} X_1(p_a; q_1; p_b), \quad (4.26)$$

where X_1 is given by Eq. (2.2).

V. REMARKS

We have emphasized in this paper two important features of two-particle correlation effects in the pionization region: (i) The transverse momenta are shown to be restricted to values of the order Ω^{-1}, and their distributions are in general correlated, reflecting the MP nature of the high-energy production mechanism; (ii) these correlation effects are shown to diminish as the relative rapidity increases, with the correlation length given by the inverse of the separation between the location of the leading vacuum pole and that of the leading vacuum branch point. Although we have only demonstrated these features explicitly by using a simple and somewhat unrealistic MR model, we are confident of their generality because, as we have shown in Sec. III, they depend only on the chain structure of MPM and the structure of the J plane.

There are two sources of uncertainties which could possibly invalidate our conclusions. First, there is the complication of the secondary trajectories, some of which can lead to longer correlation lengths than the one we have considered. The generalization to include these singularities is a straightforward procedure; we associate a "correlation length" with each lower J-plane singularity contribution. However, since each "parent" trajectory yields a factorizable contribution to Δf^{12}, it will *not* lead to a $\cos\phi$ dependence that is characteristic of a MP mechanism: A term of the form $g(\kappa_1)(\Sigma_{12})^{-(\alpha_v-\alpha_M)}g(\kappa_2)$, α_M being the secondary trajectory, has a smooth $\cos\phi$ dependence and actually favors $\cos\phi=1$. The peaking effect at $\cos\phi=-1$ can only come from nonfactorizable singularities such as branch points and daughter trajectories. Our result represents a typical branch-point contribution; and the effect of a daughter trajectory has already been studied in the context of the dual-resonance model.[11] Remarkably, both results are qualitatively similar.

A more serious objection can be raised concerning the relative sign of the branch-point contribution. Under our present approximation, the diagram G always contributes a positive term; and, as we shall see shortly, this is not expected to change within a MPM even if better approximations are made. Independent of this observation, we would like to argue that the physics of short-range correlations dictates this contribution to be positive. Since secondary trajectories cannot produce the $\cos\phi=-1$ peaking phenomenon, and since our arguments leading to the $\cos\phi$ dependence of G is independent of its over-all sign, a negative branch-cut contribution will lead to a peaking at $\cos\phi=1$. If this were the case, we would no longer have "local" transverse-momentum conservation; and it would, in turn, run the danger of leading to a long-range transverse-momentum correlation, if the cut is strong enough. This is clearly unacceptable.

Coming back to the question of the branch cut in MPM, we remark that the factorization assumption for the diagram H is, strictly speaking, incorrect. This is because a ladder sum, aside from generating a Regge pole, also contains a branch-point contribution itself. As we explain in Ref. 13, this additional contribution is not included in our calculation because we have avoided the question of how the CGL equation can be solved. The term G roughly corresponds to the usual elastic Amati-Fubini-Stanghellini (AFS) contribution, and the complete branch-cut effect is the sum of G and H. For instance, it can be shown that Δf_{12} coming from G alone, when $\alpha'\neq 0$, has also an additional $(\ln\Sigma_{12})^{-1}$ factor, whereas the sum "softens" the branch cut, leading to a dependence

$$(\Sigma_{12})^{-(\alpha_v-\alpha_c)}(\ln\Sigma_{12})^{-1-\epsilon},$$

with $\epsilon>0$. However, this *will not* change the sign of the net contribution.[24] In view of the simple physical arguments presented in Sec. III, we believe that the qualitative features of our transverse-momentum correlation obtained earlier will survive the modification from H.

Of course, all our present discussions depend on the assumption that $1\geq\alpha_v>\alpha_c$. If $\alpha_c=2\alpha_v-1=\alpha_v=1$, we find that the correlation length is infinite, so that the correlation function only vanishes logarithmically: $\Delta f_{12}\sim(\ln\Sigma_{12})^{-(1+\epsilon)}$. It is generally believed that the Pomeranchon contribution has a small coefficient so that the double-Pomeranchon cut effect can probably be left out at our present experimental accuracy. Therefore, our results could represent the situation having a Pomeranchon α_v, and an effective branch cut α_c, $\alpha_v>\alpha_c$.

We would like to suggest that the above results can be used realistically to describe two-particle inclusive cross sections in the central region if *they carry exotic quantum numbers*. Our experience with the dual-resonance model suggests that, under such conditions, secondary trajectories will not contribute to the two-particle pionization region.[25] Therefore, our predictions can be tested for $(\pi^+\pi^+)$ or $(\pi^-\pi^-)$ cross sections. Of course, care has to be taken in the actual experimental analysis so that we only consider events in the pionization region. To summarize: We predict that $(\pi^+\pi^+)$ and $(\pi^-\pi^-)$ distributions have a positive correlation in the central region with a correlation length $(\alpha_v-\alpha_c)^{-1}$, which also exhibit the ten-

dency to favor $\cos\phi = -1$. For the $(\pi^+\pi^-)$ distribution, on the other hand, one would expect an additional positive contribution with a correlation length $(\alpha_v - \alpha_M)^{-1} \simeq 2$, which is nearly $\cos\phi$ independent.

If $(\alpha_v - \alpha_M)^{-1} > (\alpha_v - \alpha_c)^{-1}$,[26] it then follows that "unlike" particles will tend to have a bigger opening angle than "like" particles, in the sense defined by GGLP.[27] However, this is quite different from GGLP's original explanation since our calculation of branch cuts corresponds to a "cross section," not "wave function," symmetrization. We urge experimental tests of these speculations.

ACKNOWLEDGMENTS

We thank H. M. Fried and K. Kang for discussions on the concept of short-range correlations. Also one of us (C.-I T.) is happy to acknowledge fruitful discussions with D. Silverman during the early development of the ideas considered here.

APPENDIX A: TWO-PARTICLE DISTRIBUTION AND MULTIPERIPHERAL CHAIN

We shall first derive Eq. (2.5) following essentially the same steps of the Appendix in I. Consider a particular MP chain with $N+2$ final particles. Let the detected particle pair have momenta q_1 and q_2, and let us specify the MR amplitude T_{N+2} by a set of four-momentum transfers to the left $\{p_i\}$, $1 \leq i \leq n$, and to the right $\{k_i\}$, $1 \leq j \leq m$, and in between q_1 and q_2, Q. Whereas the contribution to the total cross section due to this $N+2$-particle state is

$$\sigma^{N+2}(p_a, p_b) = \frac{1}{2\Delta^{1/2}(s, m_a^2, m_b^2)} \int |T_{N+2}|^2 \, d\Phi^{N+2}, \tag{A1}$$

the two-particle cross section from this same configuration is

$$d\sigma^{N+2}(q_1, q_2; p_a, p_b) = \frac{d^4q_1 \delta^+(q_1^2 - \mu^2) d^4q_2 \delta^+(q_2^2 - \mu^2)}{2\Delta^{1/2}(s, m_1^2, m_2^2)} \sum_{\substack{n=1 \\ (m=N-n)}}^{N-1} \int \frac{d^4Q}{(2\pi)^{10}} \, d\Phi^n \, d\Phi^m \, |T_{N+2}|^2 . \tag{A2}$$

$d\Phi^{N+2}$, $d\Phi^n$, $d\Phi^m$ are Lorentz-invariant phase-space factors given by Eq. (A2), Eq. (A5) of I. The summation over n is due to the freedom of the location of this pair (q_1, q_2) within the MP chain. Making a MP expansion for T_{N+2}, we find

$$|T_{N+2}(p_a, p_b; \{p_i\}, \{k_i\}, q_1, q_2)|^2 = \left| \frac{T_{n+1}(p_a, -Q; \{p_i\})}{\gamma(p_n^2)} \right|^2 |\beta((Q+q_1)^2, \omega_1, Q^2)|^2 H(Q^2, \Sigma_{12})$$

$$\times |\beta(Q^2, \omega_2, (Q-q_2)^2)|^2 \left| \frac{T_{m+1}(Q, p_b; \{h_1\})}{\gamma(k_m^2)} \right|^2 . \tag{A3}$$

The two-particle distribution is obtained by summing Eq. (A2) over N. Together with the restricted sum n, they can be converted into two unrestricted sums for n and m and performed because of the factorizable nature of T_{N+2} and $d\Phi^{N+2}$. Recalling the definition of the CGL B function,

$$B_l(p_a; -Q - q_1, -Q) = \frac{1}{2} \sum_{n=1}^{\infty} \int \left| \frac{T_{n+1}(p_a, -Q; \{p_i\})}{\gamma(p_n^2)} \right|^2 d\Phi^n(p_a, -Q - q_1; \{p_i\}), \tag{A4}$$

$$B_r(Q, Q - q_2; p_b) = \frac{1}{2} \sum_{m=1}^{\infty} \int \left| \frac{T_{m+1}(Q, p_b; \{k_i\})}{\gamma(k_m^2)} \right|^2 d\Phi^m(Q - q_2, p_b; \{k_i\}), \tag{A5}$$

Eq. (2.5) then follows.

The contributions from all other diagrams can be obtained in a similar manner. First, A is simply the nonforward 2-to-2 scattering cross section

$$A = \frac{1}{(2)(2\pi)^2} \delta^4(p_a + p_b - q_1 - q_2) |\gamma(t)|^2 (s/\mu^2)^{2\alpha(t)} . \tag{A6}$$

Diagram B is given by what is essentially a CGL B function, but with both external lines being Regge poles.[23] Let it be B, and we find

$$B=\frac{1}{(2\pi)^6}|\gamma(t_1)|^2 B(p_a, p_a-q_1; p_b-q_2, p_b)|\gamma(t_2)|^2 . \tag{A7}$$

Diagrams C and D can both be expressed in terms of B_r and B_l,

$$C=\frac{1}{(2\pi)^6}|\gamma(t)H(t,\Sigma_{12})\beta(t_2,\omega_2,t_2)|^2 B_r(p_a-q_1, p_a-q_1-q_2; p_b), \tag{A8}$$

$$D=\frac{1}{(2\pi)^6}B_l(p_a; p_b-q_1-q_2, p_b-q_2)|\beta(t_1,\omega_1,t)H(t,\Sigma_{12})\gamma(t)|^2 . \tag{A9}$$

Diagrams E, F, and H involve both B_l, B_r, and B. They are respectively given by

$$E=\frac{2}{(2\pi)^6}|\gamma(t_1)|^2\int\frac{d^4Q}{(2\pi)^4}B(p_a, p_a-q_1; Q, Q+q_2)|\beta(t,\omega_2,t_2)|^2 B_r(-Q,-Q-q_2; p_b), \tag{A10}$$

$$F=\frac{2}{(2\pi)^6}\int\frac{d^4Q}{(2\pi)^4}B_l(p_a; -q_1-Q, -Q)|\beta(t_1,\omega_1,t)|^2 B(Q+q_1, Q; p_b-q_2, p_b)|\gamma(t_2)|^2 , \tag{A11}$$

and

$$H=\frac{4}{(2\pi)^{14}}\int d^4Q_1 d^4Q_2\, B_l(p_a; Q_1, -Q_3)|\beta(t_1,\omega_1,t_3)|^2 B(-Q_1, Q_3; Q_4, -Q_2)$$
$$\times|\beta(t_4,\omega_2,t_2)|^2 B_r(-Q_4, Q_2; p_b). \tag{A12}$$

APPENDIX B

For simplicity, we present here only the result for the diagram G in the correlated pionization region. We demonstrate that $G\sim(s)^{\alpha_v}f(y, q_1^{\perp 2}, q_2^{\perp 2}, \cos\phi)$ in the limit $s\to\infty$. We make use of the technique introduced in II: Changing $p'\to p_a$, $p\to p_b$, $q'\to Q-q_2$, $q''\to -Q-q_1$, $k\to q_1+q_2$, the Jacobian of the transformation is

$$\int d^4Q_1 d^4Q d^4Q_2\,\delta^4(Q_1+Q+q_1)\delta^4(Q_2-Q-q_2)$$
$$=\int ds_1' ds_2' dt_1 dt_2 J$$
$$=\int dx dz dt_1 dt_2\frac{\theta(-\Delta((\vec{q}_1^{\perp}+\vec{q}_2^{\perp})^2, (\vec{Q}^{\perp}+\vec{q}_1^{\perp})^2, (\vec{Q}^{\perp}-\vec{q}_2^{\perp})^2))}{[-\Delta((\vec{q}_1^{\perp}+\vec{q}_2^{\perp})^2, (\vec{Q}^{\perp}+\vec{q}_1^{\perp})^2, (\vec{Q}^{\perp}-\vec{q}_2^{\perp})^2)]^{1/2}}[\kappa_1+\kappa_2+2(\kappa_1\kappa_2)^{1/2}\cosh y], \tag{B1}$$

where

$$x=\frac{-p_a\cdot(Q+q_1)}{p_a\cdot(q_1+q_2)}=\frac{s_1'-t_1-m_1^2}{-u_1-u_2+2(m_1^2+\mu^2)},$$
$$z=\frac{-p_b\cdot(q_2-Q)}{p_b\cdot(q_1+q_2)}=\frac{s_2'-t_2-m_2^2}{-v_1-v_2+2(m_2^2+\mu^2)}, \tag{B2}$$

and

$$(\vec{Q}^{\perp}-\vec{q}_2^{\perp})^2=-t_2-[\kappa_1+\kappa_2+2(\kappa_1\kappa_2)^{1/2}\cosh y](x+1)z,$$
$$(\vec{Q}^{\perp}+\vec{q}_1^{\perp})^2=-t_1-[\kappa_1+\kappa_2+2(\kappa_1\kappa_2)^{1/2}\cosh y](z+1)x. \tag{B3}$$

The assumption of Pomeranchuk-pole dominance for B_l and B_r will lead to an over-all factor s^{α_v} and leave the integrand with factors which are functions of integration variables x, z, t_1, t_2 as well as scaling variables y, $q_1^{\perp}$, $q_2^{\perp}$, $\cos\phi$. The only nontrivial step involved is to demonstrate that $Q^2\equiv t$ is an implicit function of these variables. This can be proved by noting that, because of the MP assumption, we can show that

$$t\simeq -Q_{\perp}^2+(\kappa_1\kappa_2)^{1/2}e^{-y}[x(1+e^y)+1][z(1+e^y)+1]+O(1/s). \tag{B4}$$

However, conservation of transverse momenta indicates that $Q_\perp{}^2$ is determined by $(t_1, t_2, q_1^\perp, q_2^\perp, x, z, \phi)$, which are scaled variables. The distribution can easily be shown to scale also in the single fragmentation region. We shall omit the proof since the calculation is lengthy though straightforward.

APPENDIX C: EVALUATION OF THE DIAGRAM G

The technique required to evaluate (4.2) is very similar to that used in I for the single-particle distribution. We first approximate s_1, s_2 by $s_1 \simeq s_1' - u_1$, $s_2 \simeq s_2' - v_2$, and change integration variables to s_1', s_2', t and r, where $r \equiv P^2$, $P \equiv Q - q_2 + q_1$:

$$G = \frac{2}{(2\pi)^{10}} g^8 e^{-2\Omega\mu^2} \left(\frac{\Sigma_{12}}{\mu^2}\right)^{2\bar{\alpha}_0} e^{\Omega(\Sigma_{12}-2\mu^2)} G'_{\alpha_1,\alpha_2}, \tag{C1}$$

$$G'_{\alpha_1,\alpha_2} = \frac{1}{16}\int ds_1' ds_2' (s_1')^{\alpha_v}(s_2')^{\alpha_v}\left(\frac{s_1'-u_1}{s_1'}\right)^{2\bar{\alpha}_1}\left(\frac{s_2'-v_2}{s_2'}\right)^{2\bar{\alpha}_2} I(s_1', s_2'), \tag{C2}$$

$$I(s_1', s_2') = \int \frac{dt\,dr}{\sqrt{-\Delta_4}}\,\theta(-\Delta_4) e^{2\Omega t + \Omega r}. \tag{C3}$$

Δ_4 is the Gram determinant of vectors P, $q_2 - q_1$, $p_a - q_1$, and $p_b - q_2$, and $I(s_1', s_2')$ is again an integral of the form performed in I [Eq. (3.12) of I]. The identification is completed with the substitution $p' \to -P$, $q \to q_2 - q_1$, $p \to p_a - q_1$, and $k \to p_b - q_1$, so that $I(s_1', s_2')$ is given by

$$I(s_1', s_2') = 4\pi \exp[-b] \exp[a_1(s_1'/M^2) + a_2(s_2'/M^2)] \frac{\sinh[c\Delta^{1/2}(1, s_1'/M^2, s_2'/M^2)]}{c}\,\theta(\Delta^{1/2}(M^2, s_1', s_2')), \tag{C4}$$

with

$$\begin{aligned}
b &= \Omega(M^2 - v_2 - u_1) + \tfrac{1}{2}\Omega(M^2 - u_2 - v_1),\\
a_1 &= \Omega(M^2 + v_2 - u_1) + \tfrac{1}{2}\Omega(M^2 - u_2 + v_1),\\
a_2 &= \Omega(M^2 - v_2 + u_1) + \tfrac{1}{2}\Omega(M^2 + u_2 - v_1),\\
c &= \Omega\{\Delta(M^2, v_2, u_1) + \tfrac{1}{4}\Delta(M^2, u_2, v_1) + [M^2[M^2 - u_1 - u_2 - v_1 - v_2 + 2(q_2 - q_1)^2] - (u_2 - v_1)(v_2 - u_1)]\}^{1/2}.
\end{aligned} \tag{C5}$$

In arriving at (C4) and (C5), we have substituted into Eqs. (3.15) and (3.16) of I with

$$\begin{aligned}
&\Omega_l \to 2\Omega, \quad \Omega_r \to \Omega, \quad \mu^2 \to (q_2 - q_1)^2 = 4\mu^2 - \Sigma, \quad M^2 \to M^2,\\
&t_l \to t, \quad s_l' \to s_1', \quad m_1{}^2 \to u_1, \quad u_l \to u_2,\\
&t_r \to r, \quad s_r' \to s_2', \quad m_2{}^2 \to v_1, \quad u_r \to v_2.
\end{aligned} \tag{C6}$$

As in I, the s_1' and s_2' integrations can next be performed by changing variables to

$$z(1-x) = s_1'/M^2, \quad x(1-z) = s_2'/M^2, \tag{C7}$$

and Eq. (C4) becomes

$$G'_{\alpha_1,\alpha_2} = \left(\frac{\pi}{8}\right)\frac{(M^2)^{2+2\alpha_v}}{c}\exp(-b+c)\int_0^1\int_0^1 dx\,dz\,\theta(1-x-z)(1-x-z)\vartheta_{\alpha_1,\alpha_2} \times \exp\{-[(c-a_1)z + (c-a_2)x + (a_1+a_2)xz]\}, \tag{C8}$$

where

$$\vartheta_{\alpha_1,\alpha_2}(x,z) = [z(1-x)]^{\alpha_v}[x(1-z)]^{\alpha_v}\left[1 + \frac{\tau_1}{z(1-x)}\right]^{2\bar{\alpha}_1}\left[1 + \frac{\tau_2}{x(1-z)}\right]^{2\bar{\alpha}_2}, \tag{C9}$$

with

$$\tau_1 \equiv -u_1/M^2, \quad \tau_2 \equiv -v_2/M^2. \tag{C10}$$

For the restricted case of $\alpha_1, \alpha_2 = 0, \frac{1}{2}$ and $\alpha_v = 1$, we have

$$g_{\alpha_1,\alpha_2} = (M^2)^2[z(1-x) + \tau_1\delta_{\alpha_1,1/2}][x(1-z) + \tau_2\delta_{\alpha_2,1/2}],$$

and these terms can be removed by formal differentiation. The result is

$$G'_{\alpha_1,\alpha_2} = \frac{\pi}{8}\frac{(M^2)^{2+2\alpha_v}}{c}\left(\frac{d}{da_1} + \tau_1\delta_{\alpha_1,1/2}\right)\left(\frac{d}{da_2} + \tau_2\delta_{\alpha_2,1/2}\right)\left(\frac{1}{a_1+a_2}\right)\frac{d}{dc}$$

$$\times\{\exp(-b+c)[\exp(\lambda_1)E_1(\lambda_1)] + \exp(-b-c)[\exp(\lambda_2)E_1(\lambda_2)]$$

$$- \exp(-b+a_1)[\exp(\lambda_3)E_1(\lambda_3)] - \exp(-b+a_2)[\exp(\lambda_4)E_1(\lambda_4)]\}, \tag{C11}$$

where

$$E_1(\lambda) = \int_\lambda^\infty dx\, xe^{-x}, \tag{C12}$$

$$\lambda_1 = \frac{(c-a_1)(c-a_2)}{a_1+a_2}, \quad \lambda_2 = \frac{(c+a_1)(c+a_2)}{a_1+a_2}, \quad \lambda_3 = \frac{(c-a_1)(c+a_1)}{a_1+a_2}, \quad \lambda_4 = \frac{(c+a_2)(c-a_2)}{a_1+a_2}. \tag{C13}$$

The main feature of Eq. (C11) is the exponential decrease of the terms as given by the exponents

$$-b+a_1 \simeq \Omega(2v_2+v_1), \quad -b+a_2 \simeq \Omega(2u_1+u_2),$$

$$-b \pm c \simeq (-b)\left(1 \mp \{1 - (\Omega^2/4b^2)[4(2u_1+u_2)(2v_2+v_1) + 8M^2(q_2-q_1)^2]\}^{1/2}\right). \tag{C14}$$

In the regions of interest to us, we always have

$$0 < b-c \ll b-a_1,\ b-a_2,\ b+c \tag{C15}$$

together with the fact that

$$\frac{1}{x+1} < e^x E_1(x) < \frac{1}{x}, \quad x>0, \tag{C16}$$

it follows that the first term in (C11) always dominates over others.

More generally, we can scale z, x in (C8) by $(c-a_1)$ and $(c-a_2)$,

$$x' \equiv (c-a_2)x, \quad z' = (c-a_1)z, \tag{C17}$$

and we find

$$G = g^8 e^{-2\Omega\mu^2}(M^2)^{\alpha_v}(\Sigma_{12}/\mu^2)^{2\bar{\alpha}_0 - 1 - \alpha_v}\Phi_{\bar{\alpha}_1,\bar{\alpha}_2}(c, a_1, a_2, b), \tag{C18}$$

$$\Phi_{\bar{\alpha}_1,\bar{\alpha}_2} = \frac{1}{(8)(2\pi)^9}\left(\frac{M^2}{c}\right)\left[(3\Omega\lambda)\left(\frac{\mu^2}{\Sigma_{12}}\right)\right]^{-(\alpha_v+1)} e^{-b+c+\Omega(\Sigma_{12}-2\mu^2)}$$

$$\times \int_0 dx'dz'\,\theta\left(1 - \frac{x'}{c-a_2} - \frac{z'}{c-a_1}\right)\left(1 - \frac{x'}{c-a_2} - \frac{z'}{c-a_1}\right)[(c-a_1)(c-a_2)]^{\alpha_v}$$

$$\times g_{\alpha_1,\alpha_2}\left(\frac{x'}{c-a_2}, \frac{z'}{c-a_1}\right)\exp[-(x'+z'+x'z'/\lambda)]. \tag{C19}$$

In the limit

$$k_1 \gg \mu^2, \quad k_2 \gg \mu^2, \tag{C20}$$

Eq. (C19) yields

$$\Phi_{\bar{\alpha}_1,\bar{\alpha}_2} \simeq \frac{1}{(8)(2\pi)^9}\left(\frac{M^2}{c}\right)\left(\frac{3\Omega\lambda\mu^2}{\Sigma_{12}}\right)^{-(\alpha_v+1)}[\tau_1(c-a_1)]^{2\bar{\alpha}_1}[\tau_2(c-a_2)]^{2\bar{\alpha}_2}$$

$$\times\Gamma(\alpha_v - (2\bar{\alpha}_1 - 1))\Gamma(\alpha_v - (2\bar{\alpha}_2 - 1))\exp[-b+c+\Omega(\Sigma_{12}-2\mu^2)]. \tag{C21}$$

APPENDIX D: FACTORIZATION OF DIAGRAM H

By solving a generalized CGL equation,[23] one can show that B has Regge behavior

$$B(-Q_1, Q_3; Q_4, -Q_2) \simeq \left[\frac{(Q_4 - Q_1)^2}{(Q_4 + Q_3)^2} \right]^{2\alpha(t_3)} A(Q_3; Q_4) \left[\frac{(Q_3 - Q_2)^2}{(Q_3 + Q_4)^2} \right]^{2\alpha(t_4)}, \tag{D1}$$

where

$$A(Q_3; Q_4) \simeq g^2 \frac{|\gamma(t_3)|^2}{|\gamma(\mu^2)|^2} [(Q_3 + Q_4)]^{\alpha_v(0)} \frac{|\gamma(t_4)|^2}{|\gamma(\mu^2)|^2} . \tag{D2}$$

In the strong-ordering approximation, we have

$$\left[\frac{(Q_4 - Q_1)^2}{(Q_4 + Q_3)^2} \right] \simeq \left[\frac{(p_b - Q_1)^2}{(p_b + Q_3)^2} \right], \quad \left[\frac{(Q_3 - Q_2)^2}{(Q_3 + Q_4)^2} \right] \simeq \left[\frac{(p_a - Q_2)^2}{(p_a + Q_4)^2} \right], \tag{D3}$$

and

$$(Q_3 + Q_4)^2 \simeq \frac{(p_a + Q_4)^2 (p_b + Q_3)^2}{(p_a + p_b)^2} , \tag{D4}$$

so that

$$B(-Q_1, Q_3; Q_4, -Q_2) \simeq g^2 (s_{ab})^{-\alpha_v} \frac{|\gamma(t_3)|^2}{|\gamma(\mu^2)|^2} \left[\frac{(Q_1 - p_b)^2}{(Q_3 + p_b)^2} \right]^{2\alpha(t_3)} [(Q_3 + p_b)^2]^{\alpha_v} [(p_a + Q_4)^2]^{\alpha_v}$$
$$\times \left[\frac{(p_a - Q_2)^2}{(p_a + Q_4)^2} \right]^{2\alpha(t_4)} \frac{|\gamma(t_4)|^2}{|\gamma(\mu^2)|^2} . \tag{D5}$$

Substituting (D5) into (A12) and using (4.1) and (2.2), we obtain

$$H = g^2 (s_{ab})^{-\alpha_v} X_1(p_a; q_1; p_b) X_1(p_a; q_2; p_b) . \tag{D6}$$

It then follows from (1.11), (2.1), and (2.3) that the contribution to f_{ab}^{12} due to the diagram H is precisely (in the central region)

$$f_{ab}^{12}(H) = f^1(q_1^\perp) f^2(q_2^\perp) . \tag{D7}$$

---

*Work supported in part by the U. S. Atomic Energy Commission.

[1] "Multiperipheralism" refers to a class of dynamical approximations used in handling multiparticle production at high energies. Many different versions of MPM are listed in Refs. 2–4. For definiteness, we adopt here the interpretation of multiperipheralism given by M. L. Goldberger [Erice Summer School, 1969 (unpublished)]. The common ingredients of all these models are (i) a linear chain structure with each "cell" function describing the details of the short-range correlation, and (ii) transverse-momentum cutoffs provided by dampings in momentum transfers defined by the linear chain. Our analysis here mainly depends on these two properties, together with an experimental input setting the scale of the transverse-momentum distribution. However, in order to make our discussion precise, we shall adopt the Chew-Goldberger-Low model as the standard MPM. With proper interpretations, the CGL model can be thought to include all existing MPM as special cases. In this connection, see also G. F. Chew, T. Rogers, and D. R. Snider, Phys. Rev. D 2, 765 (1970).

[2] L. Bertocchi, S. Fubini, and M. Tonin, Nuovo Cimento 25, 626 (1962); D. Amati, A. Stanghellini, and S. Fubini, *ibid.* 26, 896 (1962).

[3] G. F. Chew, M. L. Goldberger, and F. Low, Phys. Rev. Letters 22, 208 (1969); G. F. Chew and C. DeTar, Phys. Rev. 180, 1577 (1969); A. H. Mueller and I. J. Muzinich, Ann. Phys. (N.Y.) 57, 20 (1970); 57, 500 (1970); M. Ciafaloni, C. DeTar, and M. N. Misheloff, Phys. Rev. 188, 2522 (1969); M. L. Goldberger, C.-I Tan, and J. M. Wang, *ibid.* 184, 1920 (1969); D. Silverman and C.-I Tan, Phys. Rev. D 1, 3479 (1970); S. Pinsky and W. I. Weisberger, *ibid.* 2, 1640 (1970). G. F. Chew and A. Pignotti, Phys. Rev. 176, 2112 (1968).

[4] J. S. Ball and G. Marchesini, Phys. Rev. 188, 2209 (1969); 188, 2508 (1969); G. F. Chew and W. R. Frazer, *ibid.* 181, 1914 (1969); L. Caneschi and A. Pignotti, *ibid.* 180, 1525 (1969); I. G. Halliday and L. M. Saunders, Nuovo Cimento 60A, 177 (1969).

[5] D. Silverman and C.-I Tan, Nuovo Cimento 2A, 489 (1971) (hereafter referred to as I).

[6] D. Silverman and C.-I Tan, Phys. Rev. D 3, 991 (1971) (hereafter referred to as II); see also N. F. Bali, A. Pignotti, and D. Steele, *ibid.* 3, 1167 (1971); C. DeTar, *ibid.* 3, 128 (1971); K. Wilson, Acta. Phys. Austriaca 17, 37 (1963).

[7]Experimental values of Ω can be found in K. J. Foley *et al.*, Phys. Rev. Letters 11, 425 (1963); 11, 503 (1963) [in units of $(\mathrm{GeV}/c)^{-2}$] $\pi^+p \sim 8.9$, $\pi^-p \sim 9.7$, $\kappa^+p \sim 7$, $\kappa^-p \sim 10$, $pp \sim 10$, $\bar{p}p \sim 12$. A single exponential fit is adequate for $|t| \simeq q_\perp^2 \lesssim 0.5\ (\mathrm{GeV}/c)^2$, where the cross sections usually drop from $t = 0$ by several decades. It has been pointed out by A. D. Krisch [Phys. Rev. Letters 19, 1149 (1967)] that further structure exists in the p-p reaction at larger $|t|$ values, the slope parameter decreases from 10 to 3.45 for $1 \leq |t| \leq 4$. Since we are describing effects due to regions where cross sections are supposed to be "large," the relevant parameter is thus the former, where more than 90% of the elastic events take place. As we shall discuss later, the corresponding region of interest to us for inclusive reactions is again $|q_\perp^2| \leq 0.5\ (\mathrm{GeV}/c)^2$.

[8]A. H. Mueller, Phys. Rev. D 2, 2963 (1970); for a generalization, see also H. Abarbanel, Phys. Letters 34B, 67 (1971).

[9]H. P. Stapp, Phys. Rev. D 3, 3177 (1971); C.-I Tan, *ibid.* 4, 2412 (1971); J. C. Polkinghorne (unpublished).

[10]N. F. Bali, G. F. Chew, and A. Pignotti, Phys. Rev. Letters 19, 614 (1967); see also T. W. Kibble, Phys. Rev. 131, 2282 (1963); K. A. Ter-Martirosyan, Zh. Eksp. Teor. Fiz. 44, 341 (1963) [Sov. Phys. JEPT 17, 233 (1963)]; F. Zachariasen and G. Zweig, Phys. Rev. 160, 1322 (1967).

[11]Two-particle distribution has been studied using the dual-resonance model (DRM) by C. Jen, K. Kang, P. Shen, and C.-I Tan, Phys. Rev. Letters 27, 458 (1971); Ann. Phys. (N.Y.) (to be published). Kinematics of two-particle distributions are discussed in detail in these articles. See also, A. Bassetto, M. Toller, and L. Sertorio, CERN Report No. CERN-Th-1326, 1971 (unpublished) for a general discussion.

[12]For the single-particle distribution, see, for instance, C.-I Tan in *Springer Tracts in Modern Physics; Ergebnisse der Exacten Naturwissenschaften,* edited by G. Höhler (Springer, Berlin, 1971), Vol. 60, pp. 91–106.

[13]This approximation is, in general, inaccurate. It involves replacing the whole solution of the CGL equation by contributions from the first few eigenvalues, i.e., keeping only the leading poles. The rationale for the approach is that we are then able to avoid the task of having to solve the actual MP equation; and it has been used successfully in phenomenological analyses (Ref. 19). In the present situation, our approximation corresponds to representing the branch cut of an amplitude by the AFS cut. Since the output poles of MR equations in general already include contributions from every term of ladder sums (including the single- and two-particle rungs), it is not clear how the effect of "nonadjacent" production is to be incorporated. Arbitrarily adding the first few terms of the ladder sum to the leading poles definitely will commit "double counting." Without touching the details of the MPM, we do not believe our approximation can be significantly improved.

[14]R. Feynman, Phys. Rev. Letters 23, 1415 (1969); J. Benecke, T. T. Chou, C. N. Yang, and E. Yen, Phys. Rev. 188, 2159 (1969).

[15]Dependence of β on the Toller angle is also equivalent to a dependence on $\hat{Q}_1^\perp \cdot \hat{Q}_2^\perp \equiv \cos\phi_{12}$. However, as long as this dependence is smooth, our results on the large transverse-momentum cutoff are expected to be valid.

[16]In I, a factor of $\frac{1}{2}$ was left out in Eq. (3.16), associated with Ω_l and Ω_r. Consequently, all equations in Sec. IV of I should have Ω_l and Ω_r replaced by $\Omega_l/2$ and $\Omega_r/2$. After this replacement, our present result agrees with that of I if $\Omega = \Omega_l = \Omega_r$.

[17]L. G. Ratner *et al.*, Phys. Rev. Letters 27, 68 (1971); C. W. Akerlof *et al.*, Phys. Rev. D 3, 645 (1971).

[18]C. E. DeTar, K. Kang, C.-I Tan, and J. H. Weis, Phys. Rev. D 4, 425 (1971); see also D. Gordon and G. Veneziano, *ibid.* 1, 2116 (1971); M. A. Virasoro, *ibid.* 1, 2834 (1971); R. C. Brower and R. E. Waltz, Nuovo Cimento (to be published).

[19]L. Caneschi and A. Pignotti, Phys. Rev. Letters 22, 1219 (1969); D. Silverman and C.-I Tan, Phys. Rev. D 2, 233 (1970).

[20]K. Huang and G. Segrè, Phys. Rev. Letters 27, 1095 (1971).

[21]D. Freedman, E. Jones, F. Low, and J. Young, Phys. Rev. Letters 26, 1197 (1971).

[22]C. Jen, K. Kang, P. Shen, and C.-I Tan, Phys. Rev. Letters 27, 754 (1971).

[23]An integral equation for this B with both external lines being Regge poles has been discussed in more general terms by Chung-I Tan, Phys. Rev. D 5, 1476 (1972).

[24]W. R. Frazer and C. H. Mehta, Phys. Rev. Letters 23, 258 (1969).

[25]It is not possible to write a B_8 function without having particles 1 and 2 adjacent and yet still contribute to the central region.

[26]W. D. Shephard *et al.* Phys. Rev. Letters 28, 703 (1972); W. Ko, private communication. One finds that cross sections (after integrating transverse momenta) for $\pi^\pm + p \to \pi^- + \pi^-$ + anything and $\kappa^+ + p \to \pi^- + \pi^-$ + anything exhibit a positive correlation in the central region with a correlation length, i.e., half-width, much less than 2.

[27]G. Goldhaber, S. Goldhaber, W. Lee, and A. Pais, Phys. Rev. 120, 300 (1960).